Inorganic Chemistry

Article

pubs.acs.org/IC

Tris(phosphinoamide)-Supported Uranium–Cobalt Heterobimetallic Complexes Featuring Co → U Dative Interactions

J. Wesley Napoline,[†] Steven J. Kraft,[§] Ellen M. Matson,[§] Phillip E. Fanwick,[§] Suzanne C. Bart,*[,§] and Christine M. Thomas*[,†]

[†]Department of Chemistry, Brandeis University, 415 South Street, Waltham, Massachusetts 02454, United States

[§]Department of Chemistry, H.C. Brown Laboratory, Purdue University, West Lafayette, Indiana 47907, United States

Supporting Information

ABSTRACT: A series of tris- and tetrakis(phosphinoamide) U/Co complexes has been synthesized. The uranium precursors, (η^2-$Ph_2PN^iPr)_4U$ (**1**), (η^2-$^iPr_2PNMes)_4U$ (**2**), (η^2-$Ph_2PN^iPr)_3UCl$ (**3**), and (η^2-$^iPr_2PNMes)_3UI$ (**4**), were easily accessed via addition of the appropriate stoichiometric equivalents of $[Ph_2PN^iPr]K$ or $[^iPr_2PNMes]K$ to UCl_4 or $UI_4(dioxane)_2$. Although the phosphinoamide ligands in **1** and **4** have been shown to coordinate to U in an η^2-fashion in the solid state, the phosphines are sufficiently labile in solution to coordinate cobalt upon addition of CoI_2, generating the heterobimetallic Co/U complexes $ICo(Ph_2PN^iPr)_3U[\eta^2$-$Ph_2PN^iPr]$ (**5**), $ICo(^iPr_2PNMes)_3U[\eta^2$-$(^iPr_2PNMes)]$ (**6**), $ICo(Ph_2PN^iPr)_3UI$ (**7**), and $ICo(^iPr_2PNMes)_3UI$ (**8**). Structural characterization of complexes **5** and **7** reveals reasonably short Co–U interatomic distances, with **7** exhibiting the shortest transition metal–uranium distance ever reported (2.874(3) Å). Complexes **7** and **8** were studied by cyclic voltammetry to examine the influence of the metal–metal interaction on the redox properties compared with both monometallic Co and heterobimetallic Co/Zr complexes. Theoretical studies are used to further elucidate the nature of the transition metal–actinide interaction.

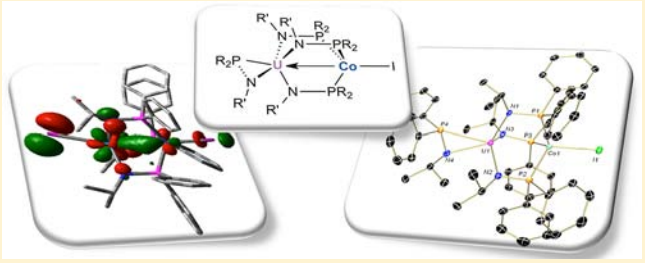

INTRODUCTION

In recent years many discoveries regarding dinuclear complexes containing direct metal–metal interactions have been made.[1−4] Interest in these compounds centers around the hypothesis that their reactivity would differ greatly from their monometallic counterparts and may yield valuable metal-based transformations. A comprehensive understanding of this class of compounds would have far-reaching implications regarding our fundamental knowledge of structure and bonding, metal surface chemistry, and cooperative metal-based catalysis. In contrast to d-block chemistry, far fewer advances have been achieved in the area of f-block metal–metal bonding. However, the large ionic radius, availability of f-orbitals, and myriad of stable oxidation states could generate heterodinuclear complexes with unique bonding properties and reactivity.

To date, few complexes that feature direct bonding between actinides, such as uranium, and transition metals have been reported. Of those, group 7 and 8 elements, including iron, ruthenium, and rhenium, are predominant.[5−9] These have been generated either by salt metathesis of U–X with anionic transition metal precursors[5,8,9] or via alkane or amine elimination from uranium alkyls or amides in the presence of a transition metal halide.[6,7] Early work by Marks described such a series of complexes, $Cp_3U–M(Cp)(CO)_2$ (M = Fe, Ru). More recently, Liddle and co-workers reported $(Tren^R)U–Ru(Cp)(CO)_2$ ($Tren^R$ = $N(CH_2CH_2NR)_3$, R = $SiMe_2{}^tBu$),[8] $(Ts^{Ar})(THF)U–Ru(Cp)(CO)_2$ (Ts^{Ar} = $HC(SiMe_2NAr)_3$; Ar = C_6H_4-4-Me, C_6H_3-3,5-Me_2),[8] $(Ts^{Ar})(THF)_nU–Re(Cp)_2$ (*n* = 1, 0; Ar = C_6H_3-3,5-Me_2),[7] and $(Tren^R)U–Re(Cp)_2$ (R = $SiMe_2{}^tBu$, $SiMe_3$),[6,9] and the nature of their metal–metal bonds was studied extensively by Gagliardi and co-workers.[10] Interactions of iron with uranium are common in ferrocenophane systems such as $[Li_2(py)_3U(fc)_3]$ (fc = $(C_5H_4)_2Fe$), reported by Ephritikhine,[11] and $[\{fc(NSiMe_2{}^tBu)_2\}_2U]^{0/+}$, $fc(NSiMe_2{}^tBu)_2U(CH_2Ph)_2$, and $[fc(NSiMe_2{}^tBu)_2U(CH_2Ph)(OEt_2)]^+$ described by Diaconescu and co-workers.[12,13] Currently, the only example of an unsupported interaction between uranium and a first row transition metal is $(Ts^{Ar})U–Co(CO)_3(PPh_3)$ (Ar = 3,5-dimethylphenyl), generated by reductive cleavage of dimeric $[Co(CO)_3(PPh_3)]_2$ by the transient trivalent $(Ts^{Xy})U$.[14]

Recently, Thomas and co-workers have developed an effective ligand framework to investigate heterobimetallic species composed of earth abundant early and late transition metals supported by LX-type phosphinoamide ligands.[15] Such early/late heterobimetallic complexes are designed to access cooperative reactivity derived from the distinct characteristics of the two transition metals. In particular, a series of Zr/Co heterobimetallic complexes featuring well-characterized metal–metal multiple bonds has been reported,[16,17] and their

Received: September 16, 2013
Published: October 10, 2013

   dx.doi.org/10.1021/ic402343q | *Inorg. Chem.* 2013, 52, 12170–12177

stoichiometric reactivity with small molecule substrates[18−22] and activity in organocatalysis has been explored.[23,24]

Due to the paucity of examples of uranium/transition metal interactions, the limited scope of synthetic methods, and the opportunity to impart unique properties to heterobimetallics using electron-rich actinides, we now focus our efforts on preparing a series of U/Co complexes that feature direct actinide−transition metal bonding. These complexes feature the shortest uranium−transition metal distance ever reported and are synthesized via a chelation/self-assembly route distinct from others reported for U-containing heterobimetallic complexes.

RESULTS AND DISCUSSION

Synthesis of Uranium Phosphinoamide Derivatives. Initial efforts were aimed at the synthesis of tris(phosphinoamide)uranium precursors, since these could be treated with cobalt salts to form the target heterobimetallics. Addition of 4 equiv of the appropriate potassium ligand salt, [Ph_2PN^iPr]K or [$^iPr_2PNMes$]K, to a THF solution of UCl_4 immediately produced color changes from green to dark yellow or orange brown, respectively. From these reaction mixtures, the uranium tetraamide species, (η^2-$Ph_2PN^iPr)_4U$ (**1**) and (η^2-$^iPr_2PNMes)_4U$ (**2**), were isolated in high yields (94% and 86%, respectively, eq 1). These homoleptic complexes were

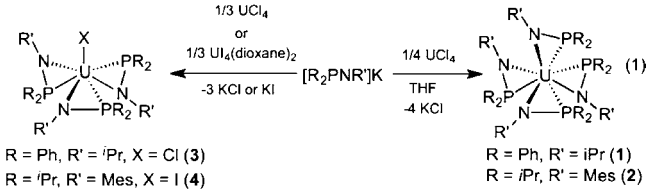

characterized by ^{1}H NMR spectroscopy and showed paramagnetically broadened and shifted spectra, with equivalent phosphinoamide ligands in solution.

The tris(phosphinoamide) uranium iodide or chloride species were synthesized using the appropriate ratio of ligand precursor. Addition of 3 equiv of [Ph_2PN^iPr]K to UCl_4 produces bright yellow (η^2-$Ph_2PN^iPr)_3UCl$ (**3**) in 96% yield (eq 1). By analogy, treatment of UI_4(dioxane)$_2$ with 3 equiv of [$^iPr_2PNMes$]K at −78 °C generates dark brown (η^2-$^iPr_2PNMes)_3UI$ (**4**) (eq 1). Analysis of **3** and **4** by ^{1}H NMR spectroscopy reveals broad, paramagnetically shifted spectra indicative of C_3 symmetric uranium species in solution.

Cooling a concentrated solution of **1** in diethyl ether to −35 °C produces crystals suitable for X-ray diffraction. Analysis of the solid state structure reveals the eight-coordinate uranium(IV) tetra(phosphinoamide) complex, (η^2-^{i}PrNP$Ph_2)_4U$, in a distorted square antiprismatic geometry (Figure 1). The molecular structure has a C_2 rotation axis, with one square of the antiprism comprised of two N2 and two P2 atoms, while the other contains two N1 and two P1 atoms. The uranium−nitrogen distances of 2.316(6) and 2.322(6) Å are similar to those observed in the homoleptic uranium(IV) amides $U(NPh_2)_4$ (U−N ∼2.27 Å),[25] $U(N(SiMe_3)_2)_4$ (U−N ∼2.29 Å),[26] and $U(N\{SiMe_2H\}_2)_4$ (U−N ∼2.28 Å).[27] The U−N bonds in **1** also closely resemble that in (PNP)UCl_3(THF) (PNP = bis[2-(diisopropylphosphino)-4-methylphenyl]-amido)[28] at 2.343(7) Å. The uranium−phosphine distances in **1** (2.8882(16) and 2.9195(16) Å) are shorter than those previously reported,[29] which may be a result of the coordinative unsaturation at U^{IV} as well as the η^2-coordination imposed by the phosphinoamide framework.

Similarly, X-ray crystallographic analysis of single crystals of **4** reveals a seven coordinate uranium center with a distorted capped trigonal antiprismatic geometry (Figure 1). The U−N distances of 2.287(4), 2.274(4), and 2.285(4) Å are shorter than those observed for **1**, as are the U−P distances of 2.8828(12), 2.8662(12), and 2.8782(12) Å. This phenomenon is believed to be the result of the increased coordinative unsaturation of the Lewis acidic uranium center.

Synthesis of Cobalt−Uranium Heterobimetallics. With the uranium phosphinoamide compounds in hand, additional studies focused on the synthesis of cobalt−uranium heterobimetallic species. In a procedure analogous to the synthesis of Zr/Co heterobimetallic complexes,[16] stirring the uranium(IV) tetra(amides) **1** and **2** with 1 equiv of CoI_2 produced noticeable color changes to red-brown and green, respectively. After workup, the products ICo($Ph_2PN^iPr)_3U[\eta^2$-$Ph_2PN^iPr]$ (**5**) and ICo($^iPr_2PNMes)_3U[\eta^2$-$^iPr_2PNMes]$ (**6**) were obtained in high yield (eq 2). The reduction of Co^{II} to Co^{I} upon treatment of

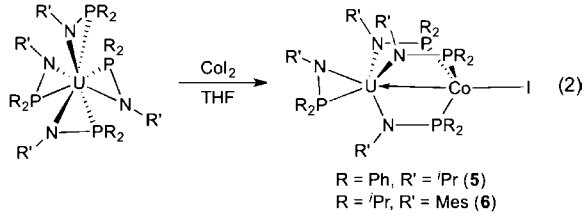

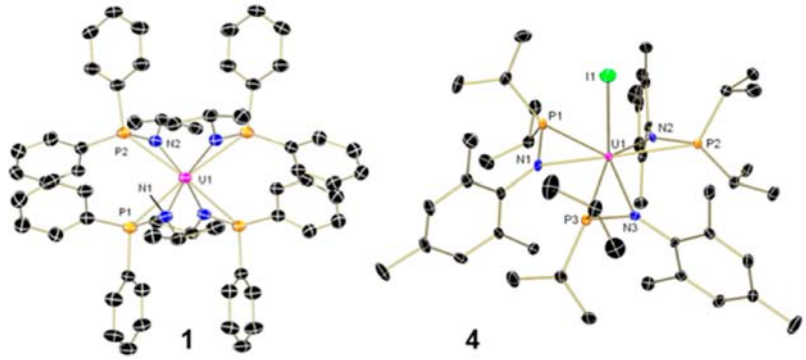

Figure 1. Molecular structures of **1** and **4** shown with 30% probability thermal ellipsoids. Hydrogen atoms and cocrystallized solvent molecules have been removed for clarity. Selected interatomic distances (Å): **1**, U1−N1 2.316(6); U1−N2 2.322(6); U1−P1 2.8882(16); U1−P2 2.9195(16); **4**, U1−N1 2.287(4); U1−N2 2.274(4); U−N3 2.285(4); U1−P1 2.8828(12); U1−P2 2.8662(12); U1−P3 2.8782(12); U1−I1 2.9775(4).

dx.doi.org/10.1021/ic402343q | Inorg. Chem. 2013, 52, 12170−12177

CoI_2 with tripodal phosphine ligands has been observed by others in monometallic systems and is thought to specifically occur in the presence of iodide.[30,31] Characterization of **5** by ^{1}H NMR spectroscopy shows 11 resonances, as is expected for two different types of phosphinoamide ligands (μ and η^2) . The ^{1}H NMR spectrum of **6** is more complicated due to inequivalent protons from hindered rotation about the N−Ar bonds as a result of the bulky mesityl groups.[32]

In order to confirm the proposed structure and investigate the cobalt−uranium interaction, X-ray crystallography was used to determine the molecular structure of **5**. Refinement of data collected from suitable crystals grown from a concentrated solution of **5** in diethyl ether at −35 °C revealed the predicted heterobimetallic species (Figure 2, Table 1). The molecular

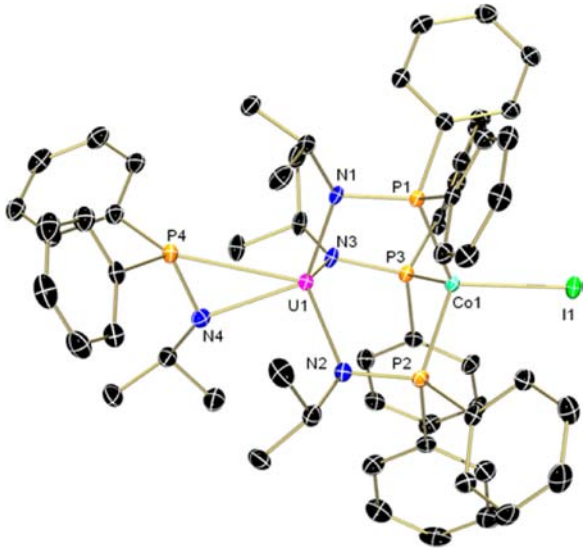

Figure 2. Molecular structure of **5** with 30% probability thermal ellipsoids. Hydrogen atoms and cocrystallized solvent molecules have been removed for clarity. Relevant interatomic distances (Å): Co−I 2.5411(8); Co−P1 2.3200(13); Co−P2 2.2710(13); Co−P3 2.2842(13); Co−U 3.0812(7); U−N1 2.273(4); U−N2 2.317(4); U−N3 2.296(4); U−N4 2.348(4); U−P4 2.8964(12).

structure features a four coordinate cobalt center in a tetrahedral geometry adjacent to a five coordinate uranium center ligated by three amido ligands and an additional η^2-phosphinoamide. The cobalt−phosphine distances range from 2.2710(13) to 2.3200(13) Å and are as expected based on the analogous zirconium−cobalt heterobimetallic ICo(MesNP^{i}Pr$_2$)$_3$ZrCl (Co−P distances 2.29−2.31 Å).[16] All angles around cobalt are within 4° of the expected 109.5° angle, supporting the tetrahedral assignment. The three uranium−nitrogen distances comprising the heterobimetallic core are 2.273(4), 2.317(4), and 2.296(4) Å, consistent with those for **1** and uranium(IV) amide species.[25−28] The uranium−cobalt distance of 3.0812(7) Å is longer than the sum of the covalent radii for uranium and cobalt (2.59 Å) if the classical Pauling covalent radii are used.[33] Others have used the revised covalent radii reported by Pyykkö when comparing interatomic distances, which gives a value of 2.81 Å for the sum of the U and Co covalent radii.[34] The U−Co distance in **5** is longer than the distance observed for the only other cobalt−uranium heterobimetallic species, (Ts^{Ar})U−Co(CO)$_3$(PPh$_3$) (Ar = 3,5-dimethylphenyl) whose U−Co distance is 2.9450(9) Å.[14]

Incorporation of cobalt into the uranium tris(phosphinoamide) derivatives, **3** and **4**, was done by treating both species with cobalt(II) iodide, generating the heterobimetallic species ICo(Ph$_2$PN^{i}Pr)$_3$UI (**7**) and ICo(^{i}Pr$_2$PNMes)$_3$UI (**8**). However, this synthetic method did not result in high isolated yields, thus a one-pot synthetic route was developed in which $UI_3(THF)_4$ was treated with 3 equiv of [Ph$_2$PN^{i}Pr]K or [^{i}Pr$_2$PNMes]K followed by CoI_2. This produced **7** (brown solid) and **8** (green solid) cleanly with higher isolated yields of 83% and 91%, respectively (eq 3).

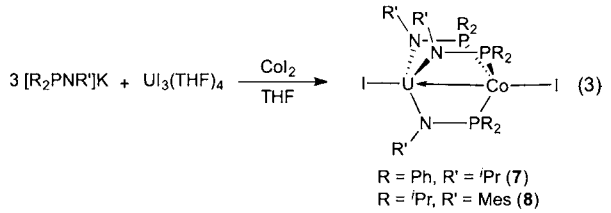

Analysis of **7** by ^{1}H NMR spectroscopy revealed a broad and paramagnetically shifted spectrum containing five resonances, indicative of a C_{3v} symmetric molecule in solution. In contrast, the spectrum for **8** showed inequivalent protons due to restricted rotation of the mesityl substituents as for **6**, and the data acquired was not useful for structural assignment.

Compound **7** was characterized by X-ray crystallography on single crystals obtained from a concentrated solution in diethyl ether at −35 °C, revealing a cobalt−uranium heterobimetallic species similar to **5** (Figure 3). In **7**, the cobalt atom is in the same tetrahedral environment as found for **5**, with Co−P bond distances ranging from 2.292(5) to 2.304(5) Å and Co angles ranging from 107.63(19)° to 111.73(16)°. The uranium center exhibits similar bonding to the bridging phosphinoamide ligands (U−N 2.250(13)−2.288(13) Å), but an iodide ligand now occupies the apical position in place of the fourth phosphinoamide found in **5**. Thus, the uranium center in **7** is four coordinate with a distorted tetrahedral geometry, which is atypical given the tendency for higher coordination numbers resulting from the large covalent radius of uranium. The cobalt−uranium distance of 2.874(3) Å is slightly longer than the sum of the covalent radii[33,34] but is shorter than that in (Ts^{Ar})U−Co(CO)$_3$(PPh$_3$).[14]

For comparison, the U−M distances of structurally characterized complexes featuring *bona fide* uranium−transition metal interactions are presented in Table S1 (Supporting Information), along with the ratio of this distance to the sum of the covalent radii of U and M (termed "formal shortness ratio (FSR)", as coined by F. Albert Cotton).[35] The FSR value takes into account differences in atomic size allowing for the direct comparison of intermetallic distances regardless of the elements involved. Thus, complexes **5** and **7** can be compared with other U/Co heterodinuclear complexes, as well as the Zr/Co analogue of **7**, ClZr(^{i}PrNPPh$_2$)$_3$CoI.[16] Compounds **5** and **7** have FSRs of 1.09 and 1.02, respectively, compared with a FSR of 0.97 for the Zr/Co analogue, illustrating the expected decrease in the strength of the metal−metal interaction between a transition metal and an actinide. Of all of the structurally characterized uranium/transition metal complexes (with FSRs ranging from 0.97 to 1.16), complex **7** features the shortest metal−uranium interatomic distance and is among the complexes with the smallest FSR.

UV−vis−NIR spectra on complexes **1**−**8** were collected in an effort to locate a metal−metal charge transfer band. The

dx.doi.org/10.1021/ic402343q | *Inorg. Chem.* 2013, 52, 12170−12177

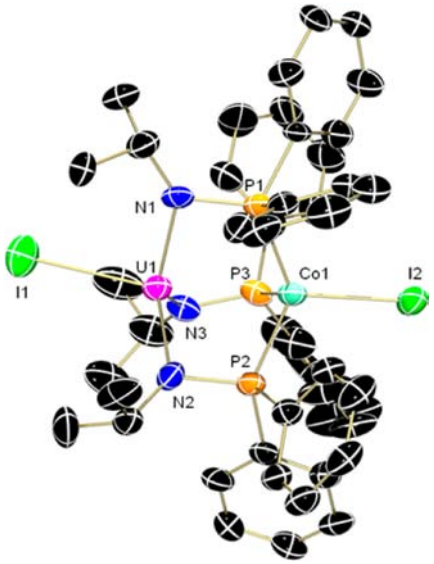

Figure 3. Molecular structure of **7** with 30% probability thermal ellipsoids. Hydrogen atoms and cocrystallized solvent molecules have been removed for clarity. Relevant interatomic distances (Å): Co−I 2.543(3); Co−P1 2.292(5); Co−P2 2.316(5); Co−P3 2.304(6); Co−U 2.874(3); U−N1 2.288(13); U−N2 2.250(13); U−N3 2.286(14); U−I 3.0213(16).

NIR region of the absorption spectra of monometallic U complexes **1**−**4** contained a number of low intensity features, as is common for uranium complexes, making it difficult to unambiguously distinguish a metal−metal charge transfer band in heterobimetallic complexes **5**−**8**. However, the NIR spectra of all four U/Co complexes contain a broad feature around ∼1300−1400 nm (ε = 50−150 M^{-1} cm^{-1}) that is not present in the monometallic species (see Supporting Information) and may be attributed to metal-to-metal charge transfer.

Cyclic Voltammetry of Cobalt−Uranium Heterobimetallic Complexes. While in general the intermetallic distance provides information about the existence of M−M interactions, additional data is usually necessary to appropriately classify such species. Electrochemistry is a useful tool in this regard, as recently demonstrated in the case of ICo(^{i}PrNPPh$_2$)$_3$ZrCl (Co−Zr distance = 2.7315(5) Å).[16] Here the metal−metal interaction led to a ∼1 V anodic shift in the reduction potential of this compound compared with its monometallic cobalt analogue, ICo(Ph$_2$PNH^{i}Pr)$_3$. This dramatic shift supported a Co → Zr dative interaction, in which the electron density at Co is withdrawn via d_{z^2}−d_{z^2} overlap with the Lewis acidic Zr center.

Based on the structural analogies to the Zr/Co complexes, a similar dative donor/acceptor interaction may be an accurate description of the bonding in complexes **7** and **8**. To support this hypothesis, **7** and **8** were analyzed using cyclic voltammetry (CV). Neither **3** nor **4** exhibited reductive features in their cyclic voltammograms within the THF solvent window, allowing all observable reductive processes to be tentatively assigned as cobalt-based. The measured reduction potentials are listed in Table 1, along with the redox potentials reported for the analogous Zr/Co heterobimetallic complexes and the monometallic cobalt tris(phosphinoamide) complex for comparison.[16]

As shown in Figure 4, the cyclic voltammogram (CV) of ICo(Ph$_2$PN^{i}Pr)$_3$UI (**7**) has a single irreversible reduction wave at −2.40 V (vs Fc/Fc$^+$).[36,37] A smaller follow-up reoxidation

Table 1. Reduction Potentials of Complexes 7 and 8 in Comparison with Analogous Co/Zr Complexes and Monometallic Complexes as Determined Using Cyclic Voltammetry[a]

compound	E_1 (V)	E_2 (V)
ICo(Ph$_2$PNH^{i}Pr)$_3$[16]	−2.49[c]	−2.66[c]
ICo(Ph$_2$PN^{i}Pr)$_3$ZrCl[16]	−1.65[b]	−1.65[b]
ICo(^{i}Pr$_2$PNMes)$_3$ZrCl[16]	−1.64[b]	−1.87[c]
ICo(Ph$_2$PN^{i}Pr)$_3$UI (**7**)	−2.40[c]	*d*
ICo(^{i}Pr$_2$PNMes)$_3$UI (**8**)	−2.19[c]	−2.83[c]

[a]Cyclic voltammetry performed in 0.4 M [Bu$_4$N][PF$_6$] in THF; working electrode, glassy carbon; reference electrode, Ag/AgNO$_3$ in THF; counter electrode, Pt^0 wire. All potentials are referenced versus the ferrocene/ferrocenium redox couple in the same solvent/electrolyte. [b]$E_{1/2}$ (reversible). A single reversible two-electron redox event is observed for ICo(Ph$_2$PN^{i}Pr)$_3$ZrCl. [c]E_{pc} (quasi-reversible) [d]Not observed.

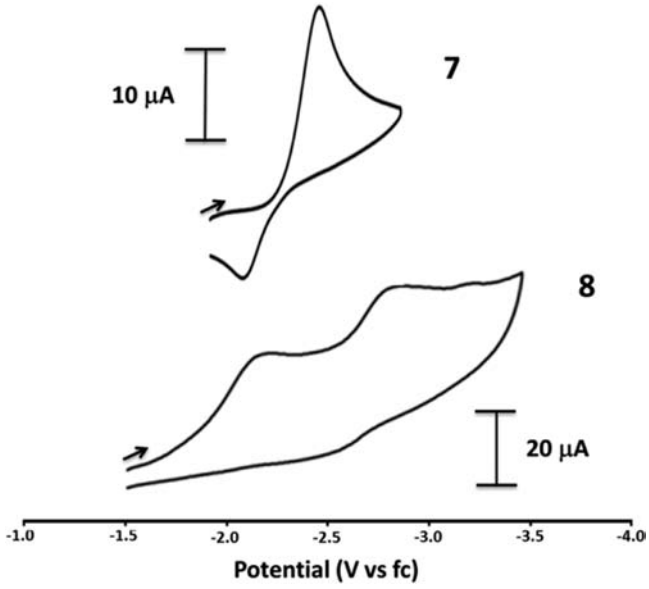

Figure 4. Reduction waves of the cyclic voltammograms of complexes **7** and **8** (2 mM analyte in 0.4 M [^{n}Bu$_4$N][PF$_6$] in THF; scan rate = 100 mV/s). Full CVs are provided in the Supporting Information.

event is observed around −2.1 V, which may be due to a quasi-reversible reduction; however, the ratio of the current intensity of these two redox events (i_{pc}/i_{pa}) does not change at faster scan rates (see Supporting Information). This reduction is assigned as a Co$^{I/0}$ process, since no reductive events were observed for the monouranium precursors, and its irreversibility is likely the result of iodide dissociation upon reduction. The Co$^{I/0}$ reduction is shifted quite modestly (∼0.1 V) from that of the monometallic Co species, ICo(Ph$_2$PNH^{i}Pr)$_3$ (−2.49 V), implying a relatively weak Co-to-U donor−acceptor interaction, particularly compared with the mild (and fully reversible) reduction of ICo(Ph$_2$PN^{i}Pr)$_3$ZrCl at −1.65 V. In contrast to the monometallic species, a second reduction event is not observed for complex **7**, although it is possible that the observed reduction is a two-electron process (similar to ICo(Ph$_2$PN^{i}Pr)$_3$ZrCl).

Two irreversible reduction waves at −2.19 and −2.83 V (vs Fc/Fc$^+$) were observed in the CV of ICo(^{i}Pr$_2$PNMes)$_3$UI (**8**), as shown in Figure 4. These events, once again, occur at more negative potentials and with less reversibility than those of the

dx.doi.org/10.1021/ic402343q | *Inorg. Chem.* 2013, 52, 12170−12177

Zr/Co counterpart, ICo(^{i}Pr$_2$PNMes)$_3$ZrCl (−1.64 and −1.87 V), but in this case, the reduction potentials are far milder than for the monometallic analogue. These data suggest a stronger Co → U interaction in **8** than in **7**, as could be expected given the more electron-donating ^{i}Pr$_2$P-substituents on the Co atom in **8**. However, since X-ray quality crystals of **8** have proven elusive, a structural confirmation of this hypothesis in the form of a shorter Co−U interatomic distance has not been confirmed experimentally.

In comparison to the data for the Zr/Co system, compounds **7** and **8** are much more difficult to reduce. Whereas Zr(IV) is a d^0 metal, uranium(IV) maintains two f electrons, making this metal center much more electron-rich. As a result, the cobalt center retains electron density, giving this species a more negative reduction potential. Thus, the U/Co system should be more reducing toward small molecules, and this will be studied in due course.

Computational Investigation. To gain further insight into the unusual uranium−cobalt interactions in complexes **7** and **8**, calculations were carried out using density functional theory (Gaussian09, DFT, BP86). The geometries of these two complexes were optimized starting from the X-ray derived coordinates of **7**, with the substituents modified to estimate a starting geometry for **8**. The optimized geometrical parameters agree reasonably well with experimental values, with the largest deviation being an overestimation of the U−Co interatomic distance by ∼0.1 Å (see Supporting Information).[38]

Nonetheless, examination of the natural frontier molecular orbitals of **7** and **8** reveal U−Co interactions (Figure 5 and Figure S10 and S11, Supporting Information). As is expected for these S = 2 combinations of U(IV) f^2 and Co(I) d^8, four of the unoccupied orbitals of **7** are centered on uranium, while the LUMO and four singly occupied molecular orbitals (SOMOs) contain contributions from both U and Co (Figure 5). Two doubly occupied molecular orbitals containing a U−Co interaction are present, one with U-amide antibonding character (21% Co, 18% U character) and one with U-amide bonding character (30% Co, 15% U character). Both of these orbitals have significant contributions from both Co and U as well as contributions from the ligand atoms. Similar molecular orbital surfaces were observed for the frontier MOs of **8**; however these representations were more complex and difficult to interpret due to substantial ligand orbital contributions (see Supporting Information).

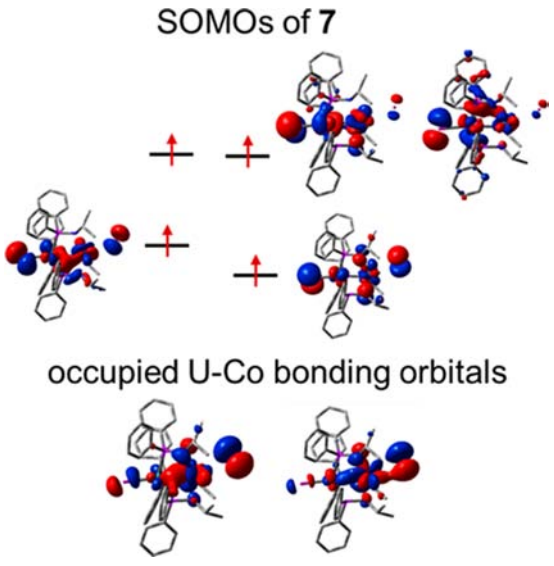

Figure 5. Calculated natural orbital representation of the SOMOs of **7** (top) and the two molecular orbitals comprising the U−Co interaction in **7**. See Supporting Information for a full molecular orbital diagram.

NBO analysis was also performed on **7** and **8**, and although NBOs corresponding to direct U−Co bonds were not present in the output, Wiberg bond indices (WBIs) suggest considerable Co−U interactions (WBI_{Co-U} = 0.47 for **7** and 0.56 for **8**; for comparison, WBI_{Co-P} = 0.5 for both complexes, shown in Table 2). Consistent with experimental results and previous trends observed in similar Zr/Co complexes,[16] the complex linked by the ^{i}Pr$_2$P-substituted ligand (**8**) is predicted to have a more substantial U−Co interaction than that in complex **7**. Given the discrepancies in natural charges computed for U and Co (Table 2), the metal−metal interactions are best thought of as dative, with the more electron-rich Co^I center donating electron density in the direction of the U^{IV} center. Notably, the natural charge on Co in the heterobimetallic complex **8** becomes more positive than that of **7** as a result of stronger donation to U.

Table 2. Computed Wiberg Bond Index (WBI), Natural Atomic Charges, and Mulliken Spin Density for Complexes 7 and 8

		natural charge		Mulliken spin density	
	Co−U WBI	U	Co	U	Co
ICo(Ph$_2$PN^{i}Pr)$_3$UI (**7**)	0.47	0.76	−0.55	2.79	1.55
ICo(^{i}Pr$_2$PNMes)$_3$UI (**8**)	0.56	0.76	−0.36	2.63	1.68

CONCLUSIONS

As described above, a series of novel phosphinoamide-supported uranium and uranium−cobalt complexes have been synthesized via an unprecedented mild chelation route. Evidence for Co → U interactions in **5**−**8** is supported by structural parameters, electrochemical potentials, and density functional theoretical calculations, the latter of which shows a weakly dative interaction between Co and U, far weaker than the interaction observed in analogous Zr/Co complexes. Donation of electron density from Co to U does, however, affect the redox activity of the Co centers, shifting the Co$^{I/0}$ couple in **7** to a slightly more positive potential than in the monometallic cobalt analogue. A more dramatic anodic shift is observed for complex **5**, suggesting that a stronger Co → U donor/acceptor interaction is present. The U center in these complexes plays the role of a Z-type metalloligand, rendering these complexes analogous to recently reported zirconium−cobalt heterobimetallic complexes that participate in a wide range of interesting and unprecedented reactivity. Future studies will focus on exploring the utility of these particular heterobimetallic U/Co complexes for small molecule activation and possible catalytic processes.

EXPERIMENTAL SECTION

General Considerations. All air- and moisture-sensitive manipulations were performed using standard Schlenk techniques or in an MBraun inert atmosphere drybox with an atmosphere of purified nitrogen. The MBraun drybox was equipped with a coldwell designed for freezing samples in liquid nitrogen as well as two −35 °C freezers

dx.doi.org/10.1021/ic402343q | Inorg. Chem. 2013, 52, 12170−12177

for cooling samples and crystallizations. Solvents for sensitive manipulations were dried and deoxygenated using literature procedures.[39] Benzene-d_6 was purchased from Cambridge Isotope Laboratories, dried with molecular sieves and sodium, and degassed by three freeze−pump−thaw cycles. Depleted uranium was purchased from Manufacturing Sciences in Oak Ridge, TN. $UI_3(THF)_4$,[40] UCl_4,[41] $UI_4(dioxane)_2$,[42] [^{i}Pr$_2$PNMes]K,[43] and [Ph$_2$PN^{i}Pr]K[43] were prepared according to literature procedures. ***Caution!*** *Depleted uranium (^{238}U) is a weak α-emitter with a half-life on the order of 10^9 years. Reactions were carried out in an inert-atmosphere glovebox using proper PPE and dosimetry monitors.*

^{1}H NMR spectra were recorded on a Varian Inova 300 spectrometer operating at 299.992 MHz. All chemical shifts are reported relative to the peak for $SiMe_4$ using ^{1}H (residual) chemical shifts of the solvent as a secondary standard. The spectra for paramagnetic molecules were obtained using an acquisition time of 0.5 s; thus the peak widths reported have an error of ±2 Hz. For paramagnetic molecules, the ^{1}H NMR data are reported with the chemical shift, followed by the peak width at half height in hertz or multiplicity, the integration value, and where possible, the peak assignment. Complexes **1**−**8** were ^{31}P NMR silent as a result of their paramagnetism. Elemental microanalyses were performed by Complete Analysis Laboratories, Inc., Parsippany, NJ. Solution magnetic moments were measured at room temperature using Evans' method.[44,45] Electronic absorption spectroscopic measurements were recorded at 294 K in THF in sealed 1 cm quartz cuvettes with a Jasco V-670 spectrophotometer.

(η^2-Ph$_2$PN^{i}Pr)$_4$U (1). A 20-mL scintillation vial was charged with 0.143 g (0.376 mmol) of UCl_4 and THF. While the mixture was stirred, 0.424 g (1.51 mmol) of [Ph$_2$PN^{i}Pr]K was added. Within 5 min, the reaction changes from green to dark yellow. The reaction was allowed to stir for 2 h to ensure completion. The solvent was removed *in vacuo*, and the dark yellow solid was dissolved in diethyl ether and filtered through Celite to remove KCl. The resulting dark yellow solution was dried under vacuum affording (Ph$_2$PN^{i}Pr)$_4$U (**1**) as a yellow solid. Purification was achieved by recrystallization from a concentrated solution of **1** in diethyl ether/pentane (2:1) at −35 °C (0.427 g, 0.353 mmol, 94%). X-ray quality single crystals were obtained from a concentrated solution of **1** in diethyl ether at −35 °C. Elemental Analyses for $C_{60}H_{68}N_4P_4U$: calcd, C, 59.70; H, 5.70; N, 4.64; found, C, 59.62; H, 5.64; N, 4.76. Evans' method (C_6D_6): 2.03 μB (note, solution magnetic moment is significantly lower than the spin-only value expected value for a S = 1 system (2.83 μB) but is similar to values reported for other tris(amido) U(IV) complexes).[46] ^{1}H NMR (C_6D_6, 25 °C): δ 5.17 (79 Hz, 40H, *o*-Ar-H, ^{i}Pr−CH_3), 6.43 (21 Hz, 8H, *p*-Ar-*H*), 6.51 (106 Hz, 16H, *m*-Ar-*H*), 34.18 (32 Hz, 4H, ^{i}Pr−C*H*).

(η^2-^{i}Pr$_2$PNMes)$_4$U (2). A 20-mL scintillation vial was charged with 0.099 g (0.261 mmol) of UCl_4 and THF. While the mixture was stirred, 0.301 g (1.04 mmol) of [^{i}Pr$_2$PNMes]K was added. Within 5 min, the reaction changed from green to orange-brown. The reaction was allowed to stir for 2 h to ensure completion. The solvent was removed *in vacuo*, and the orange-brown solid was dissolved in diethyl ether and filtered through Celite to remove KCl. The resulting orange-brown solution was dried under vacuum affording (^{i}Pr$_2$PNMes)$_4$U (**2**) as an orange-brown solid. Purification was achieved by recrystallization from a concentrated solution of **2** in diethyl ether/pentane (1:1) at −35 °C (0.278 g, 0.224 mmol, 86%). Elemental Analyses for $C_{60}H_{100}N_4P_4U$: calcd, C, 58.15; H, 8.13; N, 4.52; found, C, 58.23; H, 8.27; N, 4.47. Evans' method (C_6D_6): 3.16 μB (note, solution magnetic moment is significantly lower than the spin-only value expected value for a S = 1 system (2.83 μB) but is similar to values reported for other tris(amido) U(IV) complexes).[46] ^{1}H NMR (C_6D_6, 25 °C): δ −4.53 (271 Hz, 24H, CH_3), −2.35 (18 Hz, 24H, CH_3), 4.13 (54 Hz, 8H, ^{i}Pr−C*H*), 6.71 (3 Hz, 12H, *p*-CH_3), 7.31 (13 Hz, 24H, *o*-CH_3), 13.17 (12 Hz, 8H, Ar-*H*).

(η^2-Ph$_2$PN^{i}Pr)$_3$UCl (3). A 20-mL scintillation vial was charged with 0.110 g (0.289 mmol) of UCl_4 and THF. While the mixture was stirred, a THF solution of [Ph$_2$PN^{i}Pr]K (0.244 g, 0.868 mmol) was added. Within 5 min, the reaction changed from green to dark yellow. The reaction was allowed to stir for 1.5 h to ensure completion. The solvent was removed *in vacuo*, and the dark yellow solid was dissolved in diethyl ether and filtered through Celite to remove KCl. The resulting dark yellow solution was dried under vacuum affording (Ph$_2$PN^{i}Pr)$_3$UCl (**1**) as a yellow solid (0.183 g, 0.183 mmol, 63%). Elemental Analyses for $C_{45}H_{51}N_3P_3UCl$: calcd, C, 54.03; H, 5.14; N, 4.20; found, C, 54.02; H, 5.07; N, 4.18. Evans' method (C_6D_6): 1.99 μB (note, solution magnetic moment is significantly lower than the spin-only value expected value for a S = 1 system (2.83 μB) but is similar to values reported for other tris(amido) U(IV) complexes).[46] ^{1}H NMR (C_6D_6, 25 °C): δ 1.70 (d, J = 9 Hz, 12H, *o*-Ar-*H*), 5.85 (t, J = 6 Hz, 12H, *m*-Ar-*H*), 6.23 (t, J = 6 Hz, 6H, *p*-Ar-*H*), 22.50 (22 Hz, 18H, CH_3), 66.01 (38 Hz, 3H, *i*Pr−C*H*).

(η^2-^{i}Pr$_2$PNMes)$_3$UI (4). A 20-mL scintillation vial was charged with 0.081 g (0.088 mmol) of $UI_4(dioxane)_2$ and 5 mL of toluene and frozen in the glovebox coldwell at liquid N_2 temperatures. A second 20-mL scintillation vial was charged with 0.076 g (0.264 mmol) of [^{i}Pr$_2$PNMes]K and 5 mL of diethyl ether. Both of the vials were removed from the cold well, and the [^{i}Pr$_2$PNMes]K solution was added dropwise to the $UI_4(dioxane)_2$ solution upon thawing while stirring. Within 30 min, the reaction changed from orange to dark brown. The reaction was allowed to stir for 2 h to ensure completion. The solvent was removed *in vacuo*, and the brown solid was redissolved in diethyl ether and filtered through Celite to remove KI. The resulting brown solution was dried under vacuum affording (^{i}Pr$_2$PNMes)$_3$UI (**4**) as a brown solid. Purification was achieved by recrystallization from a concentrated solution of **4** in a diethyl ether/pentane (1:1) at −35 °C (0.078 g, 0.070 mmol, 80%). X-ray quality single crystals were obtained from a concentrated solution of **4** in diethyl ether at −35 °C. Elemental Analyses for $C_{45}H_{75}IN_3P_3U$: calcd, C, 48.37; H, 6.64; N, 3.84; found, C, 48.43; H, 6.77; N, 3.77. Evans' method (C_6D_6): 2.67 μB (note, solution magnetic moment is significantly lower than the spin-only value expected value for a S = 1 system (2.83 μB) but is similar to values reported for other tris(amido) U(IV) complexes).[46] ^{1}H NMR (C_6D_6, 25 °C): −6.08 (664 Hz, 18H, CH_3), 1.89 (26 Hz, 18H, CH_3), 2.48 (104 Hz, 6H, ^{i}Pr−C*H*), 6.37 (5 Hz, 9H, *p*-CH_3), 9.36 (17 Hz, 18H, CH_3), 12.70 (33 Hz, 6H, Ar).

ICo(Ph$_2$PN^{i}Pr)$_3$U[η^2-Ph$_2$PN^{i}Pr] (5). A 20-mL scintillation vial was charged with 0.305 g (0.253 mmol) of **1** and THF. While the mixture was stirred, 0.079 g (0.253 mmol) of CoI_2 was added. Upon stirring for 16 h, the reaction became red-brown. The solvent was removed *in vacuo*, and the red-brown solid was filtered over Celite in diethyl ether. The resulting red-brown solution was dried under vacuum affording ICo(Ph$_2$PN^{i}Pr)$_3$U[κ^2(Ph$_2$PN^{i}Pr)] (**5**) as a red-brown solid. Purification was achieved by recrystallization from a concentrated solution of **5** in diethyl ether at −35 °C (0.295 g, 0.212 mmol, 84%). X-ray quality single crystals were obtained from a concentrated solution of **5** in diethyl ether at −35 °C. Elemental Analyses for $C_{60}H_{68}IN_4P_4CoU$: calcd, C, 51.74; H, 4.92; N, 3.93; found, C, 52.01; H, 5.00; N, 4.08. Evans' method (C_6D_6): 3.68 μB (note, solution magnetic moment is significantly lower than the spin-only value expected value for a S = 2 system (4.90 μB), but the origin of this phenomenon is difficult to interpret given the uniformly low values observed for the U(IV) precursors). ^{1}H NMR (C_6D_6, 25 °C): δ −10.24 (679 Hz, 12H), −9.03 (72 Hz, 6H), −3.50 (434 Hz, 12H), −3.19 (442 Hz, 18H), 5.61 (18 Hz, 4H, Ar-*H*), 7.05 (6 Hz, 4H, Ar-*H*), 7.69 (t, J = 8 Hz, *p*-Ar-*H*), 13.27 (68 Hz, 9H, ^{i}Pr−CH_3), 13.37 (68 Hz, 9H, ^{i}Pr−CH_3), 35.39 (309 Hz, 3H, ^{i}Pr−C*H*), 65.53 (37 Hz, 1H, ^{i}Pr−C*H*).

ICo(^{i}Pr$_2$PNMes)$_3$U[η^2-^{i}Pr$_2$PNMes] (6). A 20-mL scintillation vial was charged with 0.305 g (0.247 mmol) of **2** and THF. While the mixture was stirred, 0.077 g (0.247 mmol) of CoI_2 was added. Upon stirring for 16 h, the reaction became dark green. The solvent was removed *in vacuo*, and the dark green solid was dissolved in diethyl ether and filtered through Celite. The resulting dark green solution was dried under vacuum affording ICo(^{i}Pr$_2$PNMes)$_3$U-[κ^2(^{i}Pr$_2$PNMes)] (**6**) as a dark green solid. Purification was obtained by recrystallization from a concentrated solution of **6** in diethyl ether at −35 °C (0.260 g, 0.182 mmol, 74%). Elemental Analyses for $C_{60}H_{100}IN_4P_4CoU$: calcd, C, 42.31; H, 4.02; N, 3.29; found, C, 42.39;

dx.doi.org/10.1021/ic402343q | *Inorg. Chem.* 2013, 52, 12170−12177

H, 4.06; N, 3.07. Evans' method (C_6D_6): 4.45 μB (note, solution magnetic moment is significantly lower than the expected value for an $S = 2$ system (4.90 μB), but the origin of this phenomenon is difficult to interpret given the uniformly low values observed for the U(IV) precursors). ^{1}H NMR (C_6D_6, 25 °C): δ δ −11.67 (58 Hz), −10.58 (33 Hz), −5.63 (21 Hz), −2.74 (37 Hz), 1.09 (56 Hz), 2.00 (19 Hz), 3.22 (57 Hz), 5.21 (32 Hz), 6.11 (130 Hz), 7.95 (5 Hz), 10.09 (29 Hz), 10.81 (141 Hz), 11.70 (14 Hz), 15.82 (15 Hz), 24.52 (55 Hz).

ICo(Ph$_2$PN^{i}Pr)$_3$UI (7). A 20-mL scintillation vial was charged with 0.183 g (0.202 mmol) of $UI_3(THF)_4$ and THF and frozen in the glovebox coldwell at liquid N_2 temperature. Upon thawing and under stirring, 0.171 g (0.606 mmol) of [Ph$_2$PN^{i}Pr]K was added. Upon stirring for 5 min, the reaction became red-purple, and 0.063 g (0.202 mmol) of CoI_2 was added. After 16 h of stirring, the reaction was brown in color. The solvent was removed *in vacuo*, and the remaining brown solid was dissolved in diethyl ether and filtered through Celite. The resulting brown solution was dried under vacuum affording **7** as a brown solid. Purification was achieved by recrystallization from a concentrated solution of **7** in diethyl ether at −35 °C (0.112 g, 0.088 mmol, 83%). X-ray quality single crystals were obtained from a concentrated solution of **7** in diethyl ether at −35 °C. Elemental Analyses for $C_{45}H_{51}I_2N_3P_3CoU$: calcd, C, 42.30; H, 4.02; N, 3.29; found, C, 42.19; H, 4.13; N, 3.16. Evans' method (C_6D_6): 4.93 μB. ^{1}H NMR (C_6D_6, 25 °C): δ −5.83 (38 Hz, 6H, *p*-Ar-*H*), −4.70 (286 Hz, 12H, Ar-*H*), 14.45 (36 Hz, 12H, Ar-*H*), 23.67 (43 Hz, 18H, ^{i}Pr−C*H*$_3$), 76.21 (84 Hz, 3H, ^{i}Pr−C*H*).

ICo(^{i}Pr$_2$PNMes)$_3$UI (8). A 20-mL scintillation vial was charged with 0.183 g (0.202 mmol) of $UI_3(THF)_4$ and THF and frozen in the glovebox coldwell at liquid N_2 temperature. Upon thawing and under stirring, 0.171 g (0.606 mmol) of [^{i}Pr$_2$PNMes]K was added. Upon stirring for 5 min, the reaction became red-purple, and 0.063 g (0.202 mmol) of CoI_2 was added. After 16 h of stirring, the reaction was dark green in color. The solvent was removed *in vacuo*, and the dark green solid was extracted into diethyl ether and filtered through Celite. The resulting dark green solution was dried under vacuum affording **8** as a dark green solid. Purification was achieved by recrystallization from a concentrated solution of **8** in diethyl ether at −35 °C (0.125 g, 0.096 mmol, 91%). Elemental Analyses for $C_{45}H_{75}I_2N_3P_3CoU$: calcd, C, 41.52; H, 5.81; N, 3.23; found, C, 41.42; H, 5.78; N, 3.16. Evans' method (C_6D_6): 4.92 μB. ^{1}H NMR (C_6D_6, 25 °C): δ −64.10 (158 Hz), −16.25 (38 Hz), −11.22 (247 Hz), −7.40 (16 Hz), −4.87 (237 Hz), −3.78 (50 Hz), −1.49 (9 Hz), 4.39 (51 Hz), 7.28 (8 Hz), 7.99 (365 Hz), 12.32 (9 Hz), 19.01 (27 Hz), 23.95 (15 Hz), 25.00 (66 Hz), 42.31 (50 Hz).

X-ray Crystallography. Single crystals for X-ray diffraction were coated with poly(isobutylene) oil in a glovebox and quickly transferred to the goniometer head of a Rigaku Rapid II image plate diffractometer equipped with a MicroMax002+ high intensity copper X-ray source with confocal optics. Preliminary examination and data collection were performed with Cu Kα radiation (λ = 1.54184 Å). Cell constants for data collection were obtained from least-squares refinement. The space group was identified using the program XPREP.[47] The structures were solved using the structure solution program PATTY in DIRDIFF99.[48] Refinement was performed on a LINUX PC using SHELX-97.[47] The data were collected at a temperature of 150(1) K.

Computational Details. All calculations were performed using Gaussian09, ver. E.01,[49] for the Linux operating system. Density functional theory calculations were carried out using a combination of Becke's 1988 gradient-corrected exchange functional[50] and Perdew's 1986 electron correlation functional[51] (BP86). For open shell systems, unrestricted wave functions were used in energy calculations. A mixed-basis set was employed, using the LANL2TZ(f) triple-ζ basis set with effective core potentials for cobalt and iodine,[52−55] the Stuttgart RLC basis set with effective core potentials for uranium,[56] Gaussian09's internal 6-311+G(d) for atoms bonded directly to the metal centers (nitrogen, phosphorus), and Gaussian09's internal LANL2DZ basis set (equivalent to D95V[57]) for carbon and hydrogen. Starting with crystallographically determined geometries, when available, the geometries were optimized to a minimum, followed by analytical frequency calculations to confirm that no imaginary frequencies were present. Natural bond orbital calculations were performed using NBO 3.1 as implemented in Gaussian09.[58] Orbital compositions were determined using a script provided by Dr. Jason Keith (Los Alamos National Laboratory).

Electrochemistry. Cyclic voltammetry measurements were carried out in a glovebox under a dinitrogen atmosphere in a one-compartment cell using a CH Instruments electrochemical analyzer. A glassy carbon electrode and platinum wire were used as the working and auxiliary electrodes, respectively. The reference electrode was Ag/$AgNO_3$ in THF. Solutions (THF) of electrolyte (0.40 M [^{n}Bu$_4$N][PF_6]) and analyte (2 mM) were also prepared in the glovebox.

■ ASSOCIATED CONTENT

Ⓢ Supporting Information

Full cyclic voltammograms of **7** and **8**, UV−vis−NIR data for complexes **1**−**8**, full table of relevant interatomic distances and angles in complexes **5** and **7**, crystallographic data for **1**, **4**, **5**, and **7** in CIF format, and additional computational details. This material is available free of charge via the Internet at http://pubs.acs.org.

■ AUTHOR INFORMATION

Corresponding Authors

*E-mail: thomasc@brandeis.edu.

*E-mail: sbart@purdue.edu.

Author Contributions

The manuscript was written through contributions of all authors. All authors have given approval to the final version of the manuscript. J.W.N. and S.J.K. contributed equally.

Notes

The authors declare no competing financial interest.

■ ACKNOWLEDGMENTS

The authors are grateful for financial support from Brandeis University and Purdue University for initial funding of this project. This work was also partially funded by the U.S. Department of Energy under Award No. DE-SC0004019 (C.M.T.). C.M.T. is also grateful for a 2011 Sloan Research Fellowship. S.C.B. is a Cottrell Scholar funded by the Research Corporation. The authors also thank Dr. Jason Keith for insightful discussion regarding the computational work.

■ REFERENCES

(1) Cooper, B. G.; Napoline, J. W.; Thomas, C. M. *Catal. Rev.: Sci. Eng.* **2012**, *54*, 1−40.

(2) Stephan, D. W. *Coord. Chem. Rev.* **1989**, *95*, 41−107.

(3) Wheatley, N.; Kalck, P. *Chem. Rev.* **1999**, *99*, 3379−3420.

(4) Gade, L. H. *Angew. Chem., Int. Ed.* **2000**, *39*, 2658−2678.

(5) Sternal, R. S.; Marks, T. J. *Organometallics* **1987**, *6*, 2621−2623.

(6) Gardner, B. M.; McMaster, J.; Moro, F.; Lewis, W.; Blake, A. J.; Liddle, S. T. *Chem.—Eur. J.* **2011**, *17*, 6909−6912.

(7) Patel, D.; King, D. M.; Gardner, B. M.; McMaster, J.; Lewis, W.; Blake, A. J.; Liddle, S. T. *Chem. Commun.* **2011**, *47*, 295−297.

(8) Gardner, B. M.; Patel, D.; Cornish, A. D.; McMaster, J.; Lewis, W.; Blake, A. J.; Liddle, S. T. *Chem.—Eur. J.* **2011**, *17*, 11266−11273.

(9) Gardner, B. M.; McMaster, J.; Lewis, W.; Liddle, S. T. *Chem. Commun.* **2009**, 2851−2853.

(10) Vlaisavljevich, B.; Miró, P.; Cramer, C. J.; Gagliardi, L.; Infante, I.; Liddle, S. T. *Chem.—Eur. J.* **2011**, *17*, 8424−8433.

(11) Bucaille, A.; Le Borgne, T.; Ephritikhine, M.; Daran, J.-C. *Organometallics* **2000**, *19*, 4912−4914.

(12) Monreal, M. J.; Carver, C. T.; Diaconescu, P. L. *Inorg. Chem.* **2007**, *46*, 7226−7228.

(13) Monreal, M. J.; Diaconescu, P. L. *Organometallics* **2008**, *27*, 1702−1706.

(14) Patel, D.; Moro, F.; McMaster, J.; Lewis, W.; Blake, A. J.; Liddle, S. T. *Angew. Chem., Int. Ed.* **2011**, *50*, 10388−10392.
(15) Thomas, C. M. *Comments Inorg. Chem.* **2011**, *32*, 14−38.
(16) Greenwood, B. P.; Forman, S. I.; Rowe, G. T.; Chen, C.-H.; Foxman, B. M.; Thomas, C. M. *Inorg. Chem.* **2009**, *48*, 6251−6260.
(17) Greenwood, B. P.; Rowe, G. T.; Chen, C.-H.; Foxman, B. M.; Thomas, C. M. *J. Am. Chem. Soc.* **2010**, *132*, 44−45.
(18) Krogman, J. P.; Foxman, B. M.; Thomas, C. M. *J. Am. Chem. Soc.* **2011**, *133*, 14582−14585.
(19) Marquard, S. L.; Bezpalko, M. W.; Foxman, B. M.; Thomas, C. M. *J. Am. Chem. Soc.* **2013**, *135*, 6018−6021.
(20) Napoline, J. W.; Bezpalko, M. W.; Foxman, B. M.; Thomas, C. M. *Chem. Commun.* **2013**, *49*, 4388−4390.
(21) Thomas, C. M.; Napoline, J. W.; Rowe, G. T.; Foxman, B. M. *Chem. Commun.* **2010**, *46*, 5790−5792.
(22) Napoline, J. W.; Krogman, J. P.; Shi, R.; Kuppuswamy, S.; Bezpalko, M. W.; Foxman, B. M.; Thomas, C. M. *Eur. J. Inorg. Chem.* **2013**, *2013*, 3874−3882.
(23) Zhou, W.; Napoline, J. W.; Thomas, C. M. *Eur. J. Inorg. Chem.* **2011**, *2011*, 2029−2033.
(24) Zhou, W.; Marquard, S. L.; Bezpalko, M. W.; Foxman, B. M.; Thomas, C. M. *Organometallics* **2013**, *32*, 1766−1772.
(25) Reynolds, J. G.; Zalkin, A.; Templeton, D. H.; Edelstein, N. M. *Inorg. Chem.* **1977**, *16*, 1090−1096.
(26) Lewis, A. J.; Williams, U. J.; Carroll, P. J.; Schelter, E. J. *Inorg. Chem.* **2013**, *52*, 7326−7328.
(27) Mansell, S. M.; Perandones, B. F.; Arnold, P. L. *J. Organomet. Chem.* **2010**, *695*, 2814−2821.
(28) Cantat, T.; Scott, B. L.; Morris, D. E.; Kiplinger, J. L. *Inorg. Chem.* **2009**, *48*, 2114−2127.
(29) Based on a 2013 search of the Cambridge Structural Database.
(30) Rose, M. J.; Bellone, D. E.; Di Bilio, A. J.; Gray, H. B. *Dalton Trans.* **2012**, *41*, 11788−11797.
(31) Sacconi, L.; Midollini, S. *J. Chem. Soc., Dalton Trans.* **1972**, 1213−1216.
(32) A similar number of inequivalent protons was not observed in the ^{1}H NMR spectrum of monometallic compound **2**. We attribute this difference to the lability of the weak U−P bonds in solution.
(33) Pauling, L. *The Nature of the Chemical Bond*, 3rd ed.; Cornell University Press: Ithaca, NY, 1960.
(34) Pyykkö, P.; Atsumi, M. *Chem.—Eur. J.* **2009**, *15*, 186−197.
(35) Cotton, F. A.; Murillo, C. A.; Walton, R. A. *Multiple Bonds Between Metal Atoms*; Springer Science and Business Media, Inc.: New York, 2005.
(36) In the full cyclic voltammogram of complex **7** (1.4 to −3.3 V), two additional redox events are observed, including an oxidation at −0.6 V and a reduction at −1.1 V (see Supporting Information). These two events are both absent in truncated scans, so they have not been included in the discussion here. The feature at −0.6 V can be attributed to a product of the irreversible reduction that occurs at low potentials, and the feature at −1.1 V can be attributed to a product of the irreversible oxidation at high potentials.
(37) While the potentials reported for the two reductive events of compound **7** are relatively similar to those reported for the monometallic $ICo(Ph_2PNH^iPr)_3$ complex, the sample of **7** used for cyclic voltammetry measurements has been characterized rigorously by combustion analysis, and no monometallic Co complex was observed in its ^{1}H NMR spectrum.
(38) We do note, however, that the computational methods used do not account for spin−orbit coupling, and more accurate methods are not available within the Gaussian09 software package.
(39) Pangborn, A. B.; Giardello, M. A.; Grubbs, R. H.; Rosen, R. K.; Timmers, F. J. *Organometallics* **1996**, *15*, 1518−1520.
(40) Clark, D. L.; Sattelberger, A. P.; Andersen, R. A. In *Inorganic Syntheses*; Cowley, A. H., Ed.;John Wiley & Sons, Inc.: Hoboken, NJ, 2007; Vol. 3, pp 307−315.
(41) Kiplinger, J. L.; Morris, D. E.; Scott, B. L.; Burns, C. J. *Organometallics* **2002**, *21*, 5978−5982.
(42) Monreal, M. J.; Thomson, R. K.; Cantat, T.; Travia, N. E.; Scott, B. L.; Kiplinger, J. L. *Organometallics* **2011**, *30*, 2031−2038.
(43) Kuppuswamy, S.; Bezpalko, M. W.; Powers, T. M.; Turnbull, M. M.; Foxman, B. M.; Thomas, C. M. *Inorg. Chem.* **2012**, *51*, 8225−8240.
(44) Evans, D. F. *J. Chem. Soc.* **1959**, 2003−2005.
(45) Sur, S. K. *J. Magn. Reson.* **1989**, *82*, 169−173.
(46) Vlaisavljevich, B.; Diaconescu, P. L.; Lukens, W. L.; Gagliardi, L.; Cummins, C. C. *Organometallics* **2013**, *32*, 1341−1352.
(47) Sheldrick, G. *Acta Crystallogr., Sect. A: Found. Crystallogr.* **2008**, *64*, 112−122.
(48) Beurskens, P. T.; Beurskens, G.; de Gelder, R.; Garcia-Granda, S.; Gould, R. O.; Smits, J. M. M. *Crystallography Laboratory*; University of Nijmegen: The Netherlands, 2008.
(49) Frisch, M. J.; Trucks, G. W.; Schlegel, H. B.; Scuseria, G. E.; Robb, M. A.; Cheeseman, J. R.; Scalmani, G.; Braone, V.; Mennucci, B.; Petersson, G. A., Eds.; Gaussian, Inc.: Wallingford, CT, et al. *Gaussian 09*, revision A.2; 2009 (see Supporting Information for full reference).
(50) Becke, A. D. *Phys. Rev. A: At. Mol. Opt. Phys.* **1988**, *38*, 3098−3100.
(51) Perdew, J. P. *Phys. Rev. B: Condens. Matter* **1986**, *33*, 8822−8824.
(52) Ehlers, A. W.; Bohme, M.; Dapprich, S.; Gobbi, A.; Hollwarth, A.; Jonas, V.; Kohler, K. F.; Stegmann, R.; Veldkamp, A.; Frenking, G. *Chem. Phys. Lett.* **1993**, *208*, 111−114.
(53) Hay, P. J.; Wadt, W. R. *J. Chem. Phys.* **1985**, *82*, 299−310.
(54) Hay, P. J.; Wadt, W. R. *J. Chem. Phys.* **1985**, *82*, 270−283.
(55) Roy, L. E.; Hay, P. J.; Martin, R. L. *J. Chem. Theory Comput.* **2008**, *4*, 1029−1031.
(56) Küchle, W.; Dolg, M.; Stoll, H.; Preuss, H. *Mol. Phys.* **1991**, *74*, 1245−1263.
(57) Dunning, T. H.; Hay, P. J. In *Modern Theoretical Chemistry*; Schaefer, H. F., Ed.; Plenum: New York, 1976; Vol. 3, pp 1−28.
(58) Glendening, E. D.; Reed, A. E.; Carpenter, J. E.; *NBO*, version 3.1.